Advanced Robotics, Vol. 21, No. 8, pp. 843–867 (2007)

Also available online - www.brill.nl/ar

Full paper

A novel paradigm for patient-cooperative control of upper-limb rehabilitation robots

MATJAŽ MIHELJ *, TOBIAS NEF and ROBERT RIENER

ETH Zurich and University of Zurich, Zurich, CH-8092 Switzerland

Received 4 July 2006; accepted 19 October 2006

Abstract—Early intervention and intensive therapy improve the outcome of neuromuscular rehabilitation. There are indications that where a patient is motivated and premeditates their movement, the recovery is more effective. Therefore, a strategy for patient-cooperative control of rehabilitation devices for upper extremities is proposed and evaluated. The strategy is based on the minimal intervention principle allowing an efficient exploitation of task space redundancies and resulting in user-driven movement trajectories. The patient's effort is taken into consideration by enabling the machine to comply with forces exerted by the user. The interaction is enhanced through a multimodal display and a virtually generated environment that includes haptic, visual and sound modalities.

Keywords: Upper limbs; rehabilitation robotics; minimum jerk; minimal intervention principle.

1. INTRODUCTION

Major disabilities require extensive rehabilitation programmes in order to treat disabled persons and prepare them for independent living. Cerebral vascular accidents such as ischemia and hemorrhagic stroke are considered the leading causes of disability with a prevalence of about 140 per 10 000 persons. Motor recovery after stroke or other pathologies is a dynamic process that usually starts with a total incapacity to move the affected limb and is followed by development of some imprecise movements. After some time these movements become more precise, but stiffness and involuntary movements may hamper the recovery process. Early intervention and intensive therapy improve the outcome of people recovering from traumatic brain or spinal cord injuries [1–3].

*To whom correspondence should be addressed. E-mail: matjaz.mihelj@robo.fe.uni-lj.si

1.1. State-of-the-art in motor rehabilitation

In a review article, Woldag and Hummelsheim [2] analyze the evidence-based physiotherapeutic concepts for improving arm and hand function in post-stroke patients. They note that the benefit of therapeutic strategies aiming at improving motor function in stroke patients has only been demonstrated on a general level, and that occupational therapy and physiotherapy improve motor function, although the operative components within the entire rehabilitation process are not yet identified. Basic neurological research suggests that repetitive motor activity forms the basis of motor learning and recovery. Even after a short period of simple motor training motocortical rearrangements occur that reflect kinematic aspects of the practiced movement. Frequent movement repetition utilizes the enormous plastic potential of the brain and appears to induce post-lesional rearrangements within its motor centers. The repetitive voluntary activation of functionally important muscle groups of the arm and hand is appropriate to improve their motor capacity significantly. Some authors also suggest that a statistically significant improvement of motor function in proximal and distal parts of the affected arm could be documented during the phase of the repetitive training of complex movements (grasping, lifting and moving a cup from one point to another). The same holds for the precision of movement and joint coordination. Such training also had a positive effect on the grip strength. In summary, the authors suggest that repetitive execution of complex movements is appropriate to support motor recovery in stroke patients and to accelerate its time course.

A major problem in the rehabilitation is posed by the currently largely still non-patient-specific methods used for the diagnosis and therapy of neuromuscular disorders. On the other hand, there is evidence that machine-delivered therapies can be effective in progressing the treatment [4]. The technology has advanced to a state where robots can be considered [5, 6]. Robotic devices are capable of reaction times far in advance of any human, which opens up the breadth of possible treatments. For people with upper-limb paralysis it is possible to consider therapies where intelligent assistance from a robot is able to provide varying degrees of compensatory movements for the affected limb. There are indications that where the patient is motivated, premeditates their movement and the therapy is intensive, the recovery is more effective. Intelligent robotic devices allow a broad scope to investigate these conditions. Furthermore, sensing that already exists within the robot can be used to provide comprehensive information about the underlying pathology.

Several groups have proposed robots to assist in the physiotherapy and rehabilitation of both the lower and upper limbs [7–9]. Devices provide a varying degree of assistance to patient's movements, ranging from no assistance to full assistance where the patient behaves passively. New control methodologies have been introduced that allow the machine to comply with forces exerted by the patient, which enables new possibilities for rehabilitation and also guarantees safety for the patient [10–12]. While many of the necessary technologies are in place to produce robot-

based rehabilitation devices with the right characteristics for rehabilitation, there is a major need to integrate these and identify the optimum modalities of exercise from the point of view of motor training. Within traditional therapy there is considerable controversy surrounding the most appropriate method of therapy and there are still insufficient data to identify clearly the benefits of these different approaches. When designing a robotic system, it is clearly important to consider the state-of-the-art of traditional therapy and develop a system that can be adapted to fit in with different approaches. The therapy should motivate the subject for the rehabilitation by activating their motor system and providing stimulus for their sensory inputs [13–15].

Based on conclusions in Woldag's review article [2] the robot-based rehabilitation device should enable frequent exercise of voluntary complex arm movements, which are repeated as long as necessary. A high frequency of exercises is relatively easy to achieve, since the robot does not suffer from tiredness. The programable nature of the robotic device also allows highly repeatable movements. The complexity of arm movements supported by the robot mostly depends on the robot kinematic structure (number and form of its degrees of freedom and the size of its segments). On the other hand, in order for the machine to comply with the voluntary activity of the patient, the device control system needs to be adequately designed. The robot behavior can be characterized in a number of ways. On the one hand, the robot, can be position controlled, and is, thus, stiff and unsusceptible to patient's voluntary activity; on the other hand, it can be compliant, thus responding to the patient's efforts. In general a rehabilitation device has to exhibit a large variety of behaviors to support a variety of patients from completely paralyzed ones to those having good voluntary control of their muscles. In order to guide patient's movements according to the task requirements, virtual constraints are usually implemented in the form of virtual tunnels [16]. A tunnel constrains the movement of the limb to the vicinity of a predefined trajectory, thus forcing the subject to follow a trajectory, that is not their own. In this paper a new control approach is proposed, which allows patients more freedom in selecting the movement trajectory, while at the same time the robot still provides the necessary support for the patients who suffer from almost complete paralysis. The control paradigm works as though the patient's hand is being towed through the environment. The patient is able to veer away from the virtual tow device within the constraints of the virtual towrope length.

1.2. Minimal intervention principle-based controller for rehabilitation robots

The complexity of upper limbs resulting from a large number of functional degrees of freedom, which enable enviable dexterity and functionality, requires advanced and relatively specific methods and devices for rehabilitation. A main issue when designing a controller for robotic rehabilitation devices is understanding how the many biomechanical degrees of freedom are coordinated to achieve a common goal. A human arm is a highly redundant mechanism. The optimal strategy in the face of uncertainty is to allow variability in redundant (task-irrelevant) dimensions.

The strategy should not enforce a desired trajectory, but rather use feedback more intelligently, correcting only those deviations that interfere with task goals. Todorov and Jordan [17] noted that whenever the task allows redundant solutions, movement duration exceeds the shortest sensorimotor delay and either the initial state of the plant is uncertain or the consequences of the control signals are uncertain, optimal performance is achieved by a feedback control law that resolves redundancy moment-by-moment using all available information to choose the best action under the circumstances. By postponing decisions regarding movement details until the last possible moment, such a control law takes advantage of the opportunities for more successful task completion that are constantly created by unpredictable fluctuations away from the average trajectory.

In a wide range of tasks, variability is not eliminated, but instead is allowed to accumulate in task-irrelevant (redundant) dimensions. The explanation of this phenomenon follows from an intuitive property of optimal feedback control that is called the minimal intervention principle: deviations from the average trajectory are corrected only when they interfere with task performance. If this principle holds and noise perturbs the system in all directions, the interplay of noise and control process will cause larger variability in task irrelevant directions. If certain deviations are not corrected, then certain dimensions of the control space are not being used. An optimal feedback controller has nothing to gain from correcting task-irrelevant dimensions, because its only concern is task performance and, by definition, such deviations do not interfere with the performance.

When considering a reaching movement, the optimal trajectory is a straight line between the initial and the target points with the minimum jerk movement profile [18]. Therefore, a rehabilitation robot might be programmed to enforce this straight line movement to the patient. However, for a patient the movement trajectory may not be as relevant as reaching the target. In this regard, the robot controller should not correct deviations from the straight line trajectory, but instead support the movement in the direction of the target.

2. METHODS

2.1. Direct kinematic model of the human arm

The kinematic chain of our interest, defined by the mechanics of the semi-exoskeleton robot ARMin (see Section 2.3 for details), contains four joint variables in the current configuration and will be extended to six with the new prototype, i.e., three for describing the shoulder ball-and-socket joint (ϑ_1, ϑ_2, ϑ_3), ϑ_4 for the elbow flexion/extension, ϑ_5 for the forearm pronation/supination and ϑ_6 for wrist flexion/extension (Fig. 1). Due to the simplified model of the human arm without the wrist ulnar/radial deviation, the kinematic chain is not redundant when considering the pose (position and orientation) of the hand. However, when only position is controlled, there is redundancy in the kinematic chain that needs to

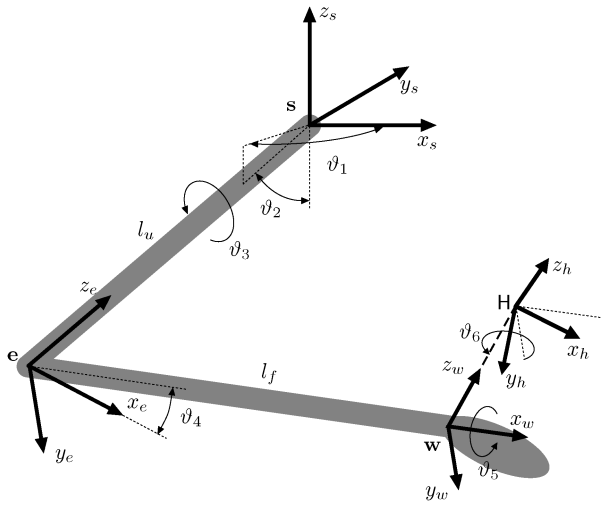

Figure 1. Simplified kinematic model of the human arm with 6 d.o.f.; l_u and l_f are the upper arm and the forearm lengths, respectively; **s**, **e** and **w** indicate shoulder, wrist and elbow positions, respectively; H is the hand pose matrix.

be properly addressed in the controller. A simple physical interpretation of the redundant degree of freedom is based on the observation that if the wrist is held fixed, the elbow is still free to swivel about a circular arc whose normal vector is parallel to the straight line connecting the shoulder and the wrist.

2.2. Control algorithm

In order to maximize the motor learning effect resulting from cortical reorganizations it is important to design a controller that guarantees balanced user involvement and increases the patient's motivation by supporting the patient's movements only as much as necessary. The implementation of a patient-cooperative control strategy requires real-time estimation of the patient's voluntary activity.

2.2.1. Robot support for reaching movements. There exists strong evidence that when moving the hand from one point in space to another healthy subjects tend to follow a straight line trajectory, minimizing the movement jerk [18], which is equal to minimizing the following cost function:

$$J(x) = \int_{t_0}^{t_\mathrm{f}} \left(\frac{\mathrm{d}^3 x}{\mathrm{d}t^3} \right)^2 \mathrm{d}t. \tag{1}$$

Some patients may lack muscle coordination and consequently they are not able to generate such optimal trajectories. However, they still might be able to produce sufficient voluntary motor effort in the direction of the target following their own trajectory, which might not be optimal in the sense of being similar to trajectories of healthy subjects. Therefore, a controller is proposed that supports the movement of

the patient's hand toward the target without predefining the trajectory, thus allowing a patient to select or modify the movement trajectory. In general, patients should be encouraged to achieve optimal movement trajectories. By predefining the maximal time allowed to complete the movement, the patients are motivated to move along the shortest possible path, thus reducing the maximal velocity needed to complete the task in time.

The basic controller proposed in this section focuses on simple point-to-point reaching movements. The movements can be position based, where the orientation of the hand is not considered, or pose based, where both position and orientation of the hand are controlled. The strategy can easily be extended to other movements, where the movement trajectory is not predefined. For more complex movements a set of intermediate reaching points (via points) can be prescribed. Between the via points the patient would still be allowed to execute his preferred trajectory. In this way it would be possible to avoid obstacles or accomplish pick-and-place tasks.

Based on the starting and the target postures, first the optimal time course trajectory is computed. The optimality is defined in terms of jerk minimization as described in (1). The result is a time-based trajectory, which only provides information on the optimal distance to the target at a certain time and not the actual reference posture in a three-dimensional (3-D) space.

First, the variable position distance to the target is defined (see Fig. 2 for details), which indicates the distance between the hand position $\mathbf{p}_\mathrm{h}(t_k)$ and the target position, $\mathbf{p}_\mathrm{t}$:

$$d_\mathrm{h}(t_k) = \|\mathbf{p}_\mathrm{t} - \mathbf{p}_\mathrm{h}(t_k)\|. \tag{2}$$

Next, a local coordinate frame is defined with the ψ_z-axis pointing from the current hand position in the direction of the target:

$$\psi_z(t_k) = \frac{\mathbf{p}_\mathrm{t} - \mathbf{p}_\mathrm{h}(t_k)}{\|\mathbf{p}_\mathrm{t} - \mathbf{p}_\mathrm{h}(t_k)\|}. \tag{3}$$

The $\psi_z(t_k)$-axis defines the main direction of the robot supporting force. The $\psi_x(t_k)$- and $\psi_y(t_k)$-axes can be selected arbitrarily. Therefore, the following definitions are used:

$$\begin{aligned} \psi_x(t_k) &= \frac{\mathbf{p}_\mathrm{h}(t_k) \times \psi_z(t_k)}{\|\mathbf{p}_\mathrm{h}(t_k) \times \psi_z(t_k)\|} \\ \psi_y(t_k) &= \psi_z(t_k) \times \psi_x(t_k). \end{aligned} \tag{4}$$

The orientation matrix of the instantaneous local coordinate frame $\Psi(t_k)$ with respect to the reference frame is then:

$$\Psi(t_k) = [\, \psi_x(t_k) \quad \psi_y(t_k) \quad \psi_z(t_k) \,]. \tag{5}$$

Similar to the variable position distance to the target the variable orientation distance to the target is introduced, which indicates the shortest rotation angle between the current hand orientation and the target orientation. First, an instantaneous axis

of rotation is computed. The rotation about this axis is the shortest rotation between the current and the target hand orientation. The instantaneous axis of rotation is denominated as $\varphi_z(t_k)$ and can be obtained using the orientation matrices of the target, R_t, and the hand, $\mathsf{R}_\mathrm{h}(t_k)$. The relations are shown in Fig. 2. An orientation error matrix is first computed as:

$$\mathsf{R}_\mathrm{e}(t_k) = \mathsf{R}_\mathrm{t}\mathsf{R}_\mathrm{h}^\mathrm{T}(t_k). \tag{6}$$

The orientation distance to the target can be calculated as:

$$\vartheta_\mathrm{h}(t_k) = \arccos \frac{\mathrm{trace}(\mathsf{R}_\mathrm{e}(t_k)) - 1}{2}, \tag{7}$$

where $\mathrm{trace}(\mathsf{R}_\mathrm{e}(t_k))$ is the sum of the diagonal elements of $\mathsf{R}_\mathrm{e}(t_k)$. The rotation axis is then:

$$\varphi_z(t_k) = \frac{1}{2\sin(\vartheta_\mathrm{h}(t_k))} \begin{bmatrix} r_{32} - r_{23} \\ r_{13} - r_{31} \\ r_{21} - r_{12} \end{bmatrix}, \tag{8}$$

where r_{ij} are elements of the matrix $\mathsf{R}_\mathrm{e}(t_k)$. The $\varphi_x(t_k)$- and $\varphi_y(t_k)$-axes that together with the $\varphi_z(t_k)$-axis constitute a local coordinate frame can be selected arbitrarily. Therefore, the following definitions are used:

$$\begin{aligned} \varphi_x(t_k) &= \frac{(\mathbf{p}_\mathrm{t} - \mathbf{p}_\mathrm{h}(t_k)) \times \varphi_z(t_k)}{\|(\mathbf{p}_\mathrm{t} - \mathbf{p}_\mathrm{h}(t_k)) \times \varphi_z(t_k)\|} \\ \varphi_y(t_k) &= \varphi_z(t_k) \times \varphi_x(t_k). \end{aligned} \tag{9}$$

The orientation matrix of the instantaneous local coordinate frame with respect to the reference frame is then:

$$\Phi(t_k) = [\, \varphi_x(t_k) \quad \varphi_y(t_k) \quad \varphi_z(t_k) \,]. \tag{10}$$

Orientation matrices for the instantaneous coordinate frames $\Psi(t_k)$ and $\Phi(t_k)$ are combined into a single transformation matrix:

$$\Upsilon(t_k) = \begin{bmatrix} \Psi(t_k) & \mathbf{0}^{3\times3} \\ \mathbf{0}^{3\times3} & \Phi(t_k) \end{bmatrix}. \tag{11}$$

Matrix $\Upsilon(t_k)$ allows transformations of vectors between the reference coordinate frame and the coordinate frames $\Psi(t_k)$ and $\Phi(t_k)$.

Next, vectors of the hand distance to the target and the hand velocity are defined. Since the shortest distances to the target are defined along $\psi_z(t_k)$ and around $\varphi_z(t_k)$, the values for distances in x and y directions are set to zero:

$$\begin{aligned} {}^\Upsilon\mathbf{x}(t_k) &= [\, \mathbf{0}^{1\times2} \quad d_\mathrm{h}(t_k) \quad \mathbf{0}^{1\times2} \quad \vartheta_\mathrm{h}(t_k) \,]^\mathrm{T}, \\ {}^\Upsilon\dot{\mathbf{x}}(t_k) &= \Upsilon^\mathrm{T}(t_k) \begin{bmatrix} \mathbf{v}_\mathrm{h}(t_k) \\ \omega_\mathrm{h}(t_k) \end{bmatrix}, \end{aligned} \tag{12}$$

where $\mathbf{0}^{1\times2} = [\, 0 \quad 0 \,]$, and $\mathbf{v}_\mathrm{h}$ and ω_h are the hand linear and angular velocities expressed in the reference coordinate frame. The superscript Υ indicates that

the vectors are expressed in the instantaneous local coordinate frames. Solving the optimization problem (1) gives a minimum jerk trajectory for the movement between the initial and final pose in the form of a fifth-order polynomial (see Ref. [18] for details):

$$\begin{aligned} {}^{\Upsilon}\mathbf{x}_{\mathrm{r}}(t_k) &= {}^{\Upsilon}\mathbf{x}(t_0)(1 - 6\tau^5 + 15\tau^4 - 10\tau^3) \\ {}^{\Upsilon}\dot{\mathbf{x}}_{\mathrm{r}}(t_k) &= {}^{\Upsilon}\mathbf{x}(t_0)\frac{30\tau^4 - 60\tau^3 + 30\tau^2}{t_f - t_0}, \end{aligned} \tag{13}$$

where t_0 and t_{f} are initial and final time, respectively, and τ is the dimensionless time, $\tau = t_k/(t_{\mathrm{f}} - t_0)$.

The same optimal trajectory can also be computed using a feedback control law [19]. Namely, the trajectory specified by (13) describes how a system should move from rest to a target location in a desired time. It is like a feedforward controller that describes the desired behavior of a system without taking into account feedback during motion. Using the approach as defined in (13) does not address the problem of changing the target position or perturbing the limb during the movement. The feedback approach monitors both the posture of the target and posture (and its derivatives) of the hand to ensure that the current desired change in hand posture is always such that it brings the hand in a minimum jerk path to the target (see Ref. [19] for details):

$$\begin{aligned} \dot{\mathsf{Q}}(t_k) &= \begin{bmatrix} 0 & 1 & 0 \\ 0 & 0 & 1 \\ -\frac{60}{(t_{\mathrm{f}}-t_k)^3} & -\frac{36}{(t_{\mathrm{f}}-t_k)^2} - \frac{9}{(t_{\mathrm{f}}-t_k)} & \end{bmatrix} \mathsf{Q}(t_k) + \begin{bmatrix} 0 \\ 0 \\ \frac{60}{(t_{\mathrm{f}}-t_k)^3} \end{bmatrix} [\, d_{\mathrm{h}}(t_0) \quad \vartheta_{\mathrm{h}}(t_0)\,] \\ {}^{\Upsilon}\mathbf{x}_{\mathrm{r}}(t_k) &= [\, \mathbf{0}^{1\times 2} \quad (d_{\mathrm{h}}(t_0) - [\,1 \quad 0\,]\mathsf{Q}^{\mathrm{T}}(t_k)\,[\,1 \quad 0 \quad 0\,]^{\mathrm{T}}) \\ &\qquad\quad \mathbf{0}^{1\times 2} \quad (\vartheta_{\mathrm{h}}(t_0) - [\,0 \quad 1\,]\mathsf{Q}^{\mathrm{T}}(t_k)\,[\,1 \quad 0 \quad 0\,]^{\mathrm{T}})\,]^{\mathrm{T}} \\ {}^{\Upsilon}\dot{\mathbf{x}}_{\mathrm{r}}(t_k) &= [\, \mathbf{0}^{1\times 2} \quad ([\,1 \quad 0\,]\mathsf{Q}^{\mathrm{T}}(t_k)\,[\,0 \quad 1 \quad 0\,]^{\mathrm{T}}) \\ &\qquad\quad \mathbf{0}^{1\times 2} \quad ([\,0 \quad 1\,]\mathsf{Q}^{\mathrm{T}}(t_k)\,[\,0 \quad 1 \quad 0\,]^{\mathrm{T}})\,]^{\mathrm{T}}. \end{aligned} \tag{14}$$

The matrix Q is a two-column matrix, where the states in the first column define the relative distance from the hand starting position and its first and second derivatives, and the states in the second column define the relative distance from the hand starting orientation and its first and second derivatives.

The actual movement of the patient's hand is then compared to the optimal trajectory and the robot support is computed based on the performance criterion presented next. The basic idea for the patient-cooperative control strategy is shown in Fig. 2. The supporting force and torque on the hand are calculated based on the error between the reference distance to the target ${}^{\Upsilon}\mathbf{x}_{\mathrm{r}}(t_k)$ and the actual distance to the target ${}^{\Upsilon}\mathbf{x}(t_k)$. The movement perpendicular to the direction of the target is damped with the force proportional to the hand velocity.

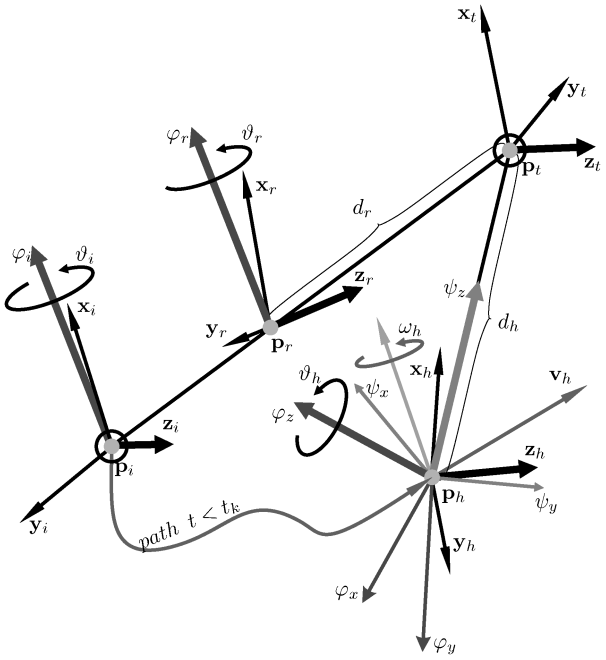

Figure 2. Graphical representation of the control strategy: starting from the initial posture at the point $\mathbf{p}_\mathrm{i}$ the subject has to reach the target posture at the point $\mathbf{p}_\mathrm{t}$; a reference distance to the target d_r is calculated using the minimum jerk optimization; a hand distance to the target d_h is compared to d_r and the supporting force, which is directed toward the target, is calculated in order to bring the hand position within the sphere located at the point $\mathbf{p}_\mathrm{t}$ with a radius d_r; a similar control strategy is implemented to control the orientation of the hand.

The generalized force on the hand, ${}^{\Upsilon}\mathbf{h}(t_k) = [\,{}^{\Upsilon}\mathbf{F}^{\mathrm{T}}(t_k) \quad {}^{\Upsilon}\tau^{\mathrm{T}}(t_k)\,]^{\mathrm{T}}$, is then computed as:

$$
\begin{aligned}
{}^{\Upsilon}\mathbf{h}(t_k) = {} & \mathsf{K}_{\mathrm{d}x}\left({}^{\Upsilon}\dot{\mathbf{x}}_{\mathrm{r}}(t_k) - {}^{\Upsilon}\dot{\mathbf{x}}(t_k)\right) \\
& - \begin{cases} \mathsf{K}_x(t_k)\left({}^{\Upsilon}\mathbf{x}_{\mathrm{r}}(t_k) - {}^{\Upsilon}\mathbf{x}(t_k)\right) & \text{if } {}^{\Upsilon}\mathbf{x}(t_k) > {}^{\Upsilon}\mathbf{x}_{\mathrm{r}}(t_k) \\ \mathbf{0} & \text{if } {}^{\Upsilon}\mathbf{x}(t_k) \leqslant {}^{\Upsilon}\mathbf{x}_{\mathrm{r}}(t_k), \end{cases}
\end{aligned}
\tag{15}
$$

where $\mathsf{K}_x(t_k)$ and $\mathsf{K}_{\mathrm{d}x}$ are the controller stiffness and damping diagonal matrices, respectively. The matrices define the values of a 6-D virtual spring-damper system attached to the hand. Although in general $\mathsf{K}_x(t_k)$ defines a 6-D stiffness, only two directions are relevant for the application—the direction of axis ψ_z and around the axis $\varphi_z(t_k)$. The stiffness in these two directions defines how much the hand pose is allowed to deviate from the reference pose. The damping part defines the viscosity of the virtual medium through which the hand is moving (by increasing the values of $\mathsf{K}_{\mathrm{d}x}$ the viscous friction on the hand increases as if, for example, the hand would be moving in water instead of air). The robot support is only active when the hand distance to the target is larger then the optimal distance to the target. The force on

the hand expressed in the reference coordinate frame is then:

$$\mathbf{h}(t_k) = \Upsilon(t_k)\,{}^{\Upsilon}\mathbf{h}(t_k). \tag{16}$$

The supporting force and torque provided by the robot are adaptive in terms of the impedance matrix $\mathsf{K}_x(t_k)$. Its value is updated in a feedback loop based on the error between the reference distance to the target ${}^{\Upsilon}\mathbf{x}_{\mathrm{r}}(t_k)$ and the actual hand distance to the target ${}^{\Upsilon}\mathbf{x}(t_k)$. A simple proportional controller with diagonal gain matrix K_0 is used to adapt $\mathsf{K}_x(t_k)$ when the error is larger then ε. A decrease of the controller stiffness is introduced through a parameter $0 < \eta_{\mathrm{p}} \ll 1$ in order to reduce active support if the patient performs well:

$$\mathsf{K}_x(t_k) = (1-\eta_{\mathrm{p}})\mathsf{K}_x(t_{k-1}) + \begin{cases} \mathsf{K}_0\,\mathrm{diag}(|{}^{\Upsilon}\mathbf{x}_{\mathrm{r}}(t_k) - {}^{\Upsilon}\mathbf{x}(t_k)|) & \text{if } {}^{\Upsilon}\mathbf{x}(t_k) - {}^{\Upsilon}\mathbf{x}_{\mathrm{r}}(t_k) > \varepsilon \\ 0 & \text{if } {}^{\Upsilon}\mathbf{x}(t_k) - {}^{\Upsilon}\mathbf{x}_{\mathrm{r}}(t_k) \leqslant \varepsilon, \end{cases} \tag{17}$$

where $\mathrm{diag}(\cdot)$ is a diagonal matrix composed of the elements of vector $\cdot$.

Figure 3 shows the force field resulting from the proposed control strategy: only the position of the hand is considered. The field is derived for a single case where the patient is able to move the hand with the optimal velocity (as computed in (13)) and only the direction of the movement varies. Therefore, no supporting force is provided if the movement is completed along the line connecting the initial and target positions.

2.2.2. Adaptive arm weight compensation. The control strategy proposed in (15) supports the movement of the hand toward the target posture. At the same time it

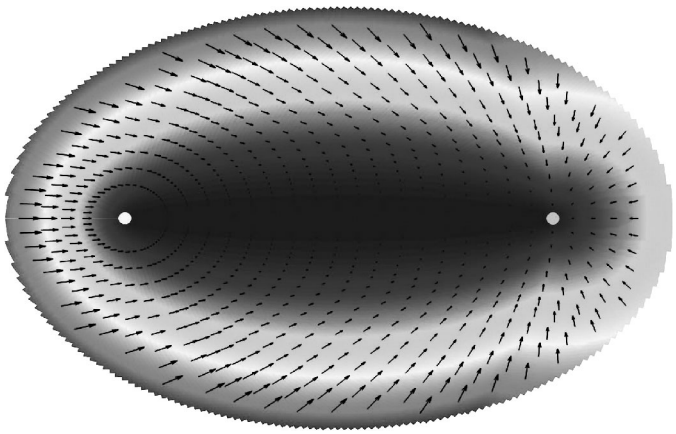

Figure 3. The force field resulting from the implementation of the control system proposed in (15). The field is derived for the case where the movement velocity generated by the patient equals the optimal velocity and only the direction of the movement varies. Left and right circles represent the initial and the target position, respectively. Black arrows show the force direction and the force magnitude is represented by grey shading; lighter outside colors represent higher forces, as indicated by the length of the arrows.

allows the subject to choose their preferred movement trajectory. The drawback of the proposed controller is that if the patient is not fit enough to support the weight of the arm, which is often the case, the movement trajectory would be shaped by the influence of gravity. Movements would generally not be directed toward the target, but the arm would first tend to move downward due to its weight. To solve this issue an adaptive gravity compensation algorithm is proposed that controls the arm weight based on the patient's performance. The weight of the robot is inherently compensated within the robot controller itself (as will be shown later).

The gravity compensation needs to be active during the entire therapy session. This means that it has to be active for reaching movements as well as when the patient is free to position his arm anywhere in space. The gravity compensation control signal is split into feedforward and feedback parts:

$$F_{\mathrm{g}}(t_k) = F_{g_{\mathrm{ff}}}(t_k) + F_{g_{\mathrm{fb}}}(t_k). \tag{18}$$

The feedforward part is always active. Its contribution adapts based on the signal from the feedback controller, which is, on the other hand, only activated during the controlled movements (i.e., when the trajectory or target pose is specified). Namely, in order to calculate the feedback contribution there is a need for a reference signal, which is obtained from the optimal trajectory for reaching tasks. The optimal vertical position of the hand, $p_{\mathrm{r}_z}(t_k)$, during the reaching movement:

$$p_{\mathrm{r}_z}(t_k) = \frac{1}{d_{\mathrm{h}}(t_0)}\big\{[\,\mathbf{0}^{1\times 2} \quad 1\,]\,(\mathbf{p}_{\mathrm{t}}(d_{\mathrm{h}}(t_0)-1) + \mathbf{p}_{\mathrm{h}}(t_0))\big\}\big\{[\,\mathbf{0}^{1\times 2} \quad 1 \quad \mathbf{0}^{1\times 3}\,]\,{}^{\Upsilon}\mathbf{x}_{\mathrm{r}}(t_k)\big\}, \tag{19}$$

is compared to the actual vertical position of the hand $p_{\mathrm{h}_z}(t_k)$ (subscript z indicates the vertical component of position). When the patient's hand position is lower than the optimal position, a supporting force is calculated opposing gravity in a similar way as if the patient's arm were suspended on ropes from the ceiling:

$$F_{g_{\mathrm{fb}}}(t_k) = \begin{cases} k_{\mathrm{p_g}}(p_{\mathrm{r}_z}(t_k) - p_{\mathrm{h}_z}(t_k)) - k_{\mathrm{v_g}} v_{\mathrm{h}_z} & \text{if } p_{\mathrm{r}_z}(t_k) > p_{\mathrm{h}_z}(t_k) \\ 0 & \text{if } p_{\mathrm{r}_z}(t_k) \leqslant p_{\mathrm{h}_z}(t_k). \end{cases} \tag{20}$$

Parameters $k_{\mathrm{p_g}}$ and $k_{\mathrm{v_g}}$ are the stiffness and the damping values for the feedback controller of the gravity support. The feedforward compensation is then updated in a feedback loop based on the calculated $F_{g_{\mathrm{fb}}}$ and a simple proportional gain k_{g_0}. A decrease of the arm weight compensation is introduced through a parameter $0 < \eta_{\mathrm{g}} \ll 1$ in order to reduce the active support if the patient performs well, meaning $F_{g_{\mathrm{fb}}}(t_k) \approx 0$. The feedforward adaptation is formulated as:

$$F_{g_{\mathrm{ff}}}(t_k) = (1-\eta_{\mathrm{g}})F_{g_{\mathrm{ff}}}(t_{k-1}) + k_{\mathrm{g}_0} F_{g_{\mathrm{fb}}}(t_k). \tag{21}$$

Due to the redundant nature of the human arm it is not possible to support its weight only at a single point (i.e., wrist). Therefore, the calculated supporting force $F_{\mathrm{g}}(t_k)$ is split into two components: one supporting the weight of the arm at the position

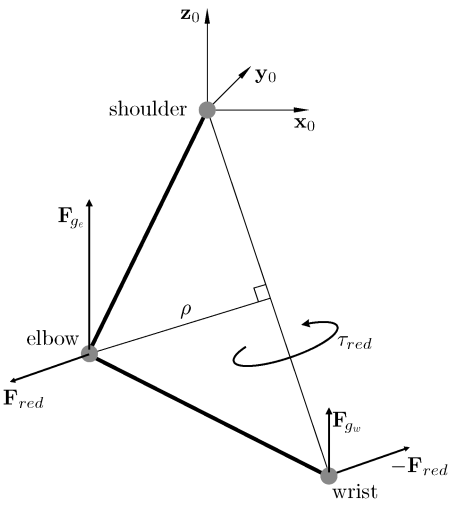

Figure 4. Schematic representation of the strategy for arm weight compensation and for controlling the arm redundancy when positioning the hand without considering its orientation. The arm weight is compensated in two points with forces $\mathbf{F}_{g_e}$ and $\mathbf{F}_{g_w}$. The redundant degree of freedom is constrained using a force, $\mathbf{F}_{red}$, acting at the elbow joint, which generates a rotation around the axis passing through the shoulder and the wrist. In order not to move the hand an opposing force of the same magnitude is applied to the wrist.

of the elbow joint (see Fig. 4):

$$F_{g_e}(t_k) = \lambda_e F_g(t_k), \tag{22}$$

and the other supporting the arm at the position of the wrist:

$$F_{g_w}(t_k) = \lambda_w F_g(t_k). \tag{23}$$

The relative distribution of the compensatory force ($\lambda_e \approx 0.7, \lambda_w \approx 0.3, \lambda_e + \lambda_w = 1$) is estimated based on the anthropometric data for the upper extremity [20]. The proposed gravity compensation strategy dynamically relieves the subject of the arm overweight, the part of the arm weight that they are not able to support by themself.

2.2.3. Redundancy control. During the reaching movements without a predefined hand orientation, the coupled robot/human arm kinematic chain is redundant. Namely, the same hand position can be achieved with an infinite number of solutions for the elbow position. However, not all arm postures are physiologically achievable or at least not equally comfortable. Therefore, a strategy for controlling the redundancy of the arm was implemented that guarantees a comfortable posture of the upper arm.

A physical interpretation of the redundant degree of freedom is based on the observation that if the wrist is held fixed, the elbow is still free to swivel about a circular arc whose normal vector is parallel to the straight line connecting the

shoulder and the wrist. Relations are shown in Fig. 4. In order to constrain the redundant degree of freedom, a torque τ_{red} is applied around the axis passing through the shoulder and the wrist. The equivalent of τ_{red} can be obtained by applying a force:

$$\mathbf{F}_{\text{red}}(t_k) = \frac{\tau_{\text{red}}(t_k)}{\rho(t_k)}, \tag{24}$$

at the elbow parallel to the elbow joint axis ($\rho(t_k)$ is the instantaneous radius of the circular swivel arc) and applying the opposite force at the wrist.

The torque $\tau_{\text{red}}(t_k)$ should be calculated in a way as to bring the arm to the most comfortable posture if there are no secondary tasks defined, e.g. obstacle avoidance. However, there exists only scarce evidence about the actual strategy that healthy subjects apply to control arm redundancy. Therefore, a simple yet efficient solution is proposed here. The empirical analysis indicates that by controlling the angle between the elbow joint axis and the horizontal plane at about $\pi/3$, a comfortable arm posture is achieved. An impedance controller with very soft stiffness settings is used to allow relatively large deviations from the reference value. This particular solution for redundancy control is not general, but can easily be replaced with a more suitable one if necessary. In therapy sessions with patients it turned out that subjects usually do not notice the difference (in a large part of the arm workspace) if the shoulder internal/external rotation is completely locked. Therefore, it is expected that the proposed strategy, which results in a comfortable posture and a soft control, would be suitable for most of the tasks.

2.2.4. Overall control system. Figure 5 shows the coupling between the high-level task controller with the virtual environment, the low-level joint space robot controller, and the controlled plant consisting of the robot and the human arm. The task-level controller, which includes the physical model of the virtual environment, the arm weight compensation and, if necessary, the redundancy control, is impedance based. The robot low-level control is admittance based. Forces computed at the task level, $\mathbf{F}_{\text{e}}$, are transformed into the desired robot joint torques, τ_{e}. These are compared to the actual interaction torques between the robot and the human arm, τ_{hs}, and the difference is fed to the joint space admittance filters, ${}^{\text{j}}\mathsf{Y}_{\text{c}}$. The outputs of ${}^{\text{j}}\mathsf{Y}_{\text{c}}$ are desired joint space velocities, which together with their integrals (desired joint space positions) constitute reference values for the local proportional-integral (PI) controllers, ${}^{\text{j}}\mathsf{D}$ (note that PI feedback of velocity is equivalent to proportional-derivative feedback of position). The robot dynamics is compensated within the local controller with ${}^{\text{j}}\hat{\mathsf{Z}}_{\text{r}}\dot{\mathbf{q}}$.

Next, the impedance, Z_{cl}, felt by the user when coupled to the robot and operating in the virtual environment with the overall impedance $\mathsf{Z}_{\text{e}} = \mathbf{F}_{\text{e}}/\mathbf{v}_{\text{h}}$ will be estimated. From relations in Fig. 5 the following equation can be derived:

$$\begin{aligned}\mathbf{v}_{\text{h}} &= \mathsf{J}\,{}^{\text{j}}\mathsf{Z}_{\text{r}}^{-1}(\tau_{\text{c}} - \mathsf{J}^{\text{T}}\mathbf{F}_{\text{h}} + {}^{\text{j}}\hat{\mathsf{Z}}_{\text{r}}\dot{\mathbf{q}}) \\ &= \mathsf{Z}_{\text{r}}^{-1}(\mathsf{J}^{-\text{T}}\tau_{\text{c}} - \mathbf{F}_{\text{h}} + \hat{\mathsf{Z}}_{\text{r}}\mathbf{v}_{\text{h}}),\end{aligned} \tag{25}$$

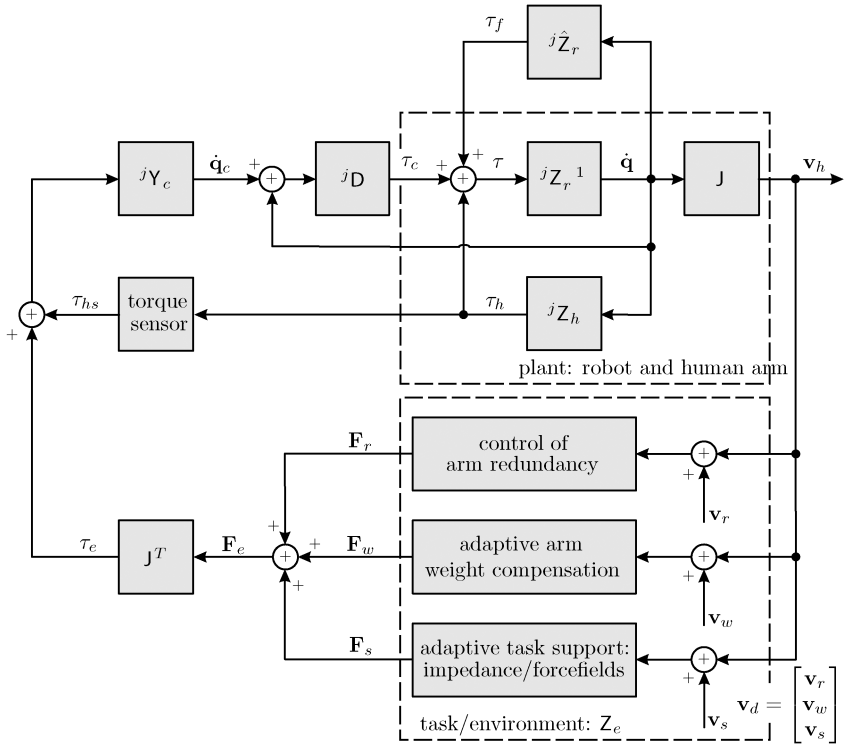

Figure 5. Block diagram of the control system with robot $^{j}Z_r$ and human arm $^{j}Z_h$ dynamics expressed in the joint space. $^{j}\hat{Z}_r$ denotes compensation of robot dynamics, J is the robot Jacobian matrix, ^{j}D is the robot joint space controller and $^{j}Y_c$ is the controller joint space admittance.

where J is the robot Jacobian matrix. $^{j}Z_r$ and Z_r denote robot impedance expressed in the joint space and in the Cartesian coordinates, respectively (hat over Z_r indicates the model used for the compensation of robot dynamics), and are related through:

$$Z_r = J^{-T\,j}Z_r J^{-1}. \tag{26}$$

In order to estimate the closed-loop impedance Z_{cl}, which is defined by the ratio of the force exerted on the human arm, $\mathbf{F}_h$, and the velocity of the human arm $\mathbf{v}_h$, we suppose without loss of generality the desired task velocity to be zero, $\mathbf{v}_d = 0$. Torque τ_c can then be determined as:

$$\begin{aligned} \tau_c|_{\mathbf{v}_d=\mathbf{0}} &= {}^{j}D[{}^{j}Y_c(-J^T Z_e \mathbf{v}_h - J^T \mathbf{F}_h) - J^{-1}\mathbf{v}_h] \\ &= J^T D[-(Y_c Z_e + I)\mathbf{v}_h - Y_c \mathbf{F}_h], \end{aligned} \tag{27}$$

where:

$$D = J^{-T\,j}D J^{-1}, \tag{28}$$

is a Cartesian space expression of robot joint space controller transfer functions and:

$$Y_c = J^{j}Y_c J^T, \tag{29}$$

is a Cartesian space expression of robot controller joint space admittance transfer functions.

With a simple algebraic manipulation of (25) and (27) it is possible to estimate the closed loop impedance Z_{cl} felt by the user as:

$$\mathsf{Z}_{\mathrm{cl}} = \frac{-\mathbf{F}_{\mathrm{h}}}{\mathbf{v}_{\mathrm{h}}} = (\mathsf{D}\mathsf{Y}_{\mathrm{c}} + \mathsf{I})^{-1}\big(\mathsf{Z}_{\mathrm{r}} - \hat{\mathsf{Z}}_{\mathrm{r}} + \mathsf{D}(\mathsf{Y}_{\mathrm{c}}\mathsf{Z}_{\mathrm{e}} + \mathsf{I})\big), \tag{30}$$

where I is an identity matrix. By increasing the gains of the local PI controllers, ${}^{\mathrm{j}}\mathsf{D} \to \infty$, the closed loop impedance simplifies to:

$$\mathsf{Z}_{\mathrm{cl}} \approx \mathsf{Z}_{\mathrm{e}} + \mathsf{Y}_{\mathrm{c}}^{-1}. \tag{31}$$

With high admittance of the robot controller Y_{c}, the closed-loop impedance Z_{cl} approaches the desired task impedance Z_{e}.

2.3. Experimental setup

ARMin, a semi-exoskeleton robot with four active degrees of freedom (three for the shoulder and one for the elbow actuation), was used for the experimental validation of the controller. Since the number of degrees of freedom is less than six, the control of hand orientation could not be experimentally validated (a new robot with 6 d.o.f. is being constructed). The robot is fixed *via* an aluminum frame at the wall with the patient sitting beneath (see Fig. 6). A vertically oriented linear motion module performs vertical shoulder rotation (flexion/extension and abduction/adduction) movements. Horizontal shoulder rotation (horizontal flexion/extension and horizontal abduction/adduction) is realized by a backlash free and back-drivable harmonic drive module attached to the slide of the linear motion module. The interconnection module connects the horizontal shoulder rotation drive with the upper arm rotary module via two hinge bearings. Internal/external shoulder rotation is achieved by a special custom-made upper arm rotary module that is connected to the upper arm via an orthotic shell. Elbow flexion/extension is realized by a harmonic drive rotary module. More details about the kinematics and mechanics of the shoulder and elbow degrees of freedom can be found in Refs [21, 22].

Figure 6 shows a healthy subject using the ARMin robot. The patient's torso is fixated to the wheelchair with straps and bands. The patient's arm is coupled to the robot via two orthotic shells: one for the upper and one for the lower arm. The fixations are characterized by an exoskeleton structure. The exoskeletal part of the robot moves the shoulder internal/external rotation, the elbow and the wrist, whereas the other two shoulder joint axes are actuated by an end-effector-based part connecting the upper arm with the wall-mounted axes.

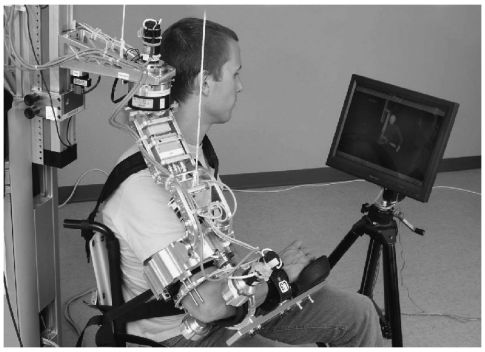

Figure 6. ARMin prototype with four active degrees of freedom that support shoulder and elbow joint movements and a healthy subject sitting in its wheelchair and looking onto the graphical display.

3. RESULTS

3.1. Simulation results

The performance of the proposed control system was first validated in a simulation study using a complete dynamic model of the ARMin robot with the human arm coupled to it. The control task was to bring the human hand from an initial to a final posture, thus controlling both position and orientation of the hand. The patient's voluntary activity was modeled as disturbance force and torque that perturb the movement from the optimal trajectory. Results of the simulation are presented in Fig. 7. The first and third plot from the top present the 3-D optimal and simulated movement trajectories for position and orientation, respectively. Due to the perturbation acting perpendicular to the movement direction, the arm posture is displaced from the optimal trajectory. However, the controller does not compensate for the disturbance by bringing the hand posture back to the optimal trajectory. The task redundancy is used and the deviations that do not interfere directly with the task execution are not compensated. The first and third plot from the top clearly indicate the minimal intervention principle operation of the controller, i.e., the position and orientation errors are not corrected to make the hand follow the optimal trajectory. Instead, a completely new trajectory is chosen that brings the hand posture with the minimum effort directly to the target, continuing from the displaced position and orientation. In this way the subject is allowed to modify the hand trajectory constantly during the movement and the controller does not interfere unless these trajectory modifications interfere with the objective (i.e., hand movement is directed away from the target). The second and fourth plot from the top show the optimal and the real distance to the target. It can be observed that although the perturbation displaces the hand posture from the optimal trajectory, the actual distance to the target closely follows the optimal distance to the target. This indicates that, due to the deviation from the shortest distance path, the movement velocity increases at least for part of the trajectory, thus penalizing such movement. In case the patient performance is better than the one predefined by the optimal trajectory, the patient

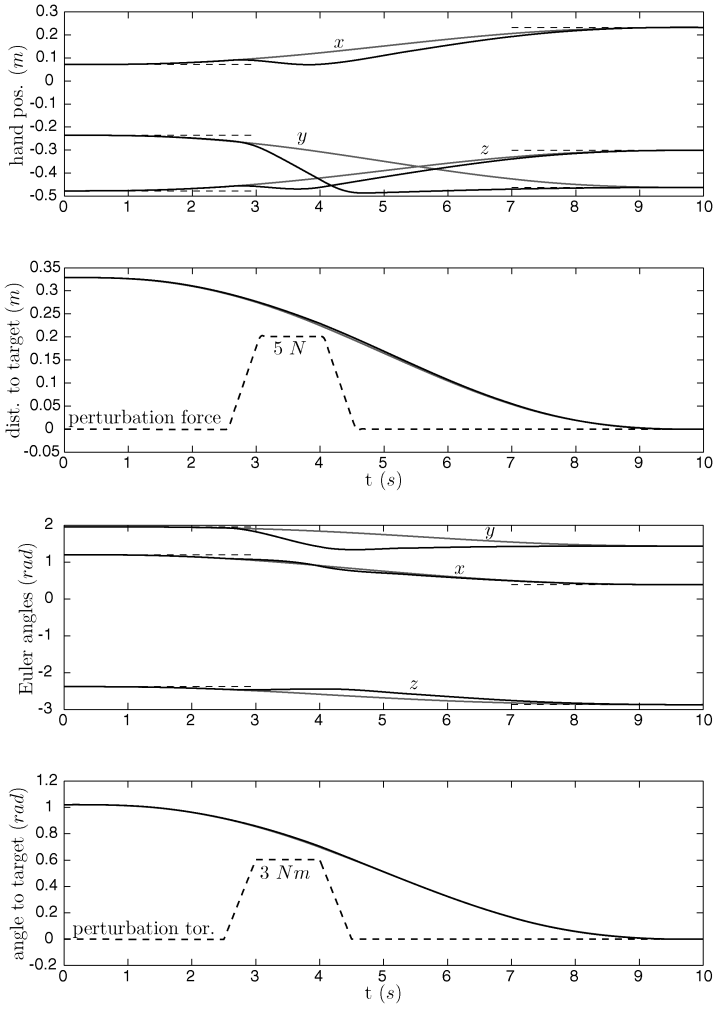

Figure 7. Results of the simulation study of the proposed control strategy based on the minimal intervention principle for the perturbed movement toward the target: position (top two plots) and orientation (bottom two plots). The first and third plot from the top present the optimal and the perturbed movement trajectories for position and orientation in 3-D space. The second and fourth plot from the top show the envelopes of disturbances, which act perpendicular to the movement direction, (dashed line, the amplitude is indicated with a number below the maximum value of the perturbation) and optimal as well as actual distance to the target. Thin grey lines indicate optimal minimum jerk trajectories. Black lines present the simulated movement trajectories.

is allowed to complete the movement in a shorter time. The controller does not interfere with such movement regardless of the chosen trajectory.

3.2. Experimental results

The proposed controller was implemented in a virtual reality scenario presented

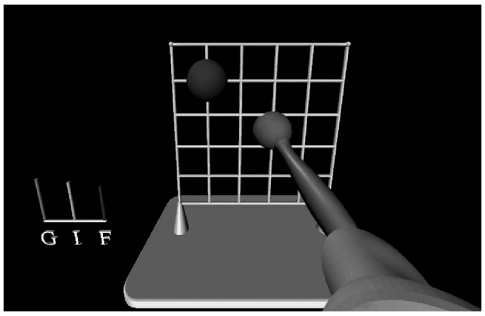

Figure 8. A virtual reality scenario for which the proposed control strategy was implemented: the task requires reaching for the ball on the grid and then moving along the grid lines toward the second ball; the bars on the left show active arm weight compensation as calculated in (21), stiffness value for the robot support as calculated in (17) and current force acting on the hand.

in Fig. 8. Only the positional part of the controller was implemented since the current robot prototype only has four active degrees of freedom. The scenario consists of three distinct movement modes. In the first mode the subject is allowed to move their arm freely in space without any robot interventions. The weight of the arm is partially compensated and the redundancy control is active. The weight compensation is adaptive and the support level is adjusted during the reaching task as defined in (21). The reaching task is the second movement mode. The goal in this mode is to reach for a ball on the grid as shown in Fig. 8. During this task the controller supports the movement with a force calculated in (15). Once the subject reaches the ball, the hand movement is constrained to the grid. The controller switches to the third operation mode where the task consists of moving along the grid lines to reach for the other ball. An additional object can be shown on the grid chasing the subject's hand, and in this way making the game more dynamic and motivating. An impedance controller is used to constrain the movement of the hand to the grid. The arm weight compensation and redundancy control are active during this task. The movement along the grid results in distinct movements in the vertical and horizontal directions, thus decoupling the complex shoulder movement in simpler ones. The three movement modes enable resting in a comfortable position (the first mode), training of reaching movements with active robot support that also allows assessment of the patient's performance (the second mode) and a game scenario for training coordinated movements, as well as assessment of performance (the third mode).

Results from the experimental validation of the control strategy for reaching movements for two different subject behaviors—active (top two plots) and passive (bottom two)—are shown in Figs 9 and 10. Active behavior indicates that the subject tries to voluntary accomplish the proposed task. On the other hand, the robot moves the subject's arm when the subject behaves passively. All passive movements were done without visual feedback so that the subject did not know the target position and, therefore, could not voluntarily contribute to the movement. Healthy

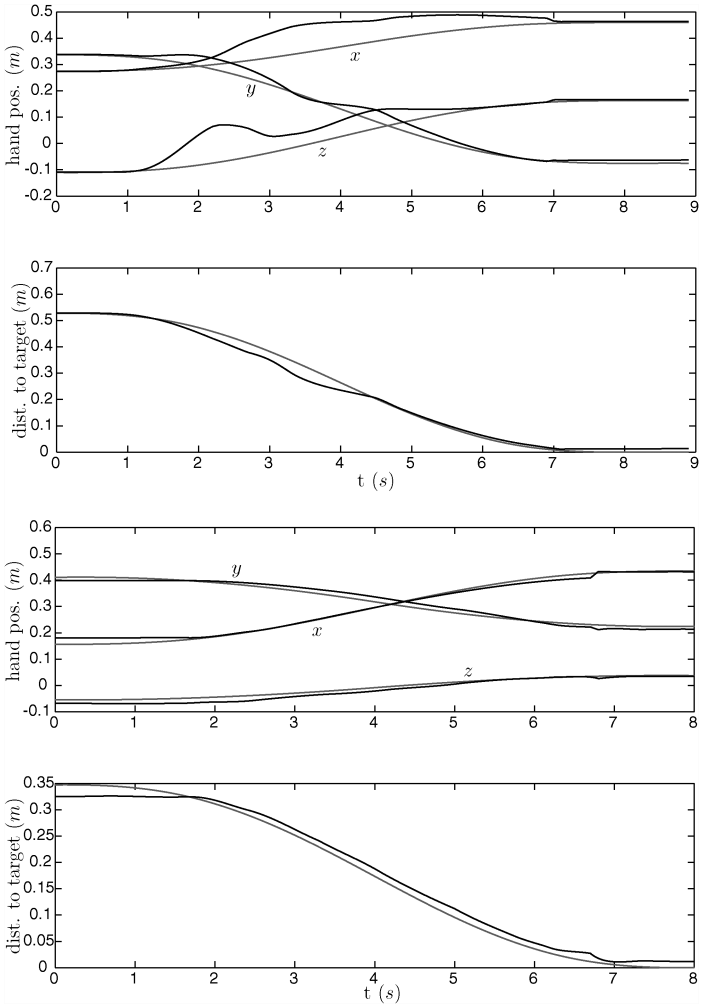

Figure 9. Hand position and distance to the target from the experimental evaluation: the top two and bottom two plots are related to active and passive subject behavior, respectively; during the active behavior the subject modifies the hand movement trajectory (as shown on the top plot) compared to the optimal trajectory (grey line); the actual distance to the target can decrease faster then the optimal distance due to the voluntary activity (second plot from the top); during the passive behavior the hand follows the optimal trajectory more closely since there is no voluntary input from the subject (third plot from the top); the actual distance to the target is always a small distance behind the optimal distance due to the proportional nature of the controller used for calculating the supportive force (bottom plot).

subjects and one stroke patient took part in the experimental sessions. To emphasize the difference between the active and passive subject behavior the presented results are for the healthy subject, i.e., it was very difficult for the stroke patient to perform the active voluntary movement due to the muscle weakness. In Fig. 9, optimal and actual positions of the hand (first and third plot from the top) and optimal and actual distances to the target (second and fourth plot from the top) are presented.

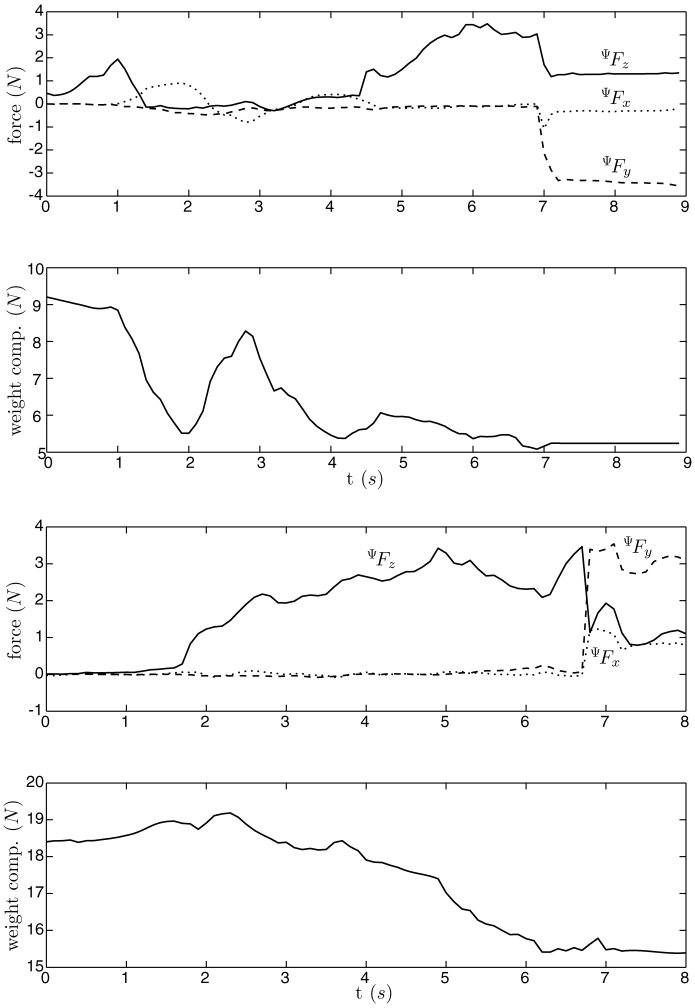

Figure 10. Supporting force (expressed in the local frame Ψ, thus z-axis pointing toward the target) and arm weight compensation from the experimental evaluation: the top two and bottom two plots are related to active and passive subject behavior, respectively; during the passive behavior there is only a force in the z direction (third plot from the top), while during the active behavior, forces in x and y directions damp the movement perpendicular to the movement toward the target (top plot); step changes at the end of the movement are the result of switching from reaching mode to the mode where the movement is constrained to the grid; during the active behavior the arm weight compensation is in general lower (second plot from the top) than during the passive behavior (bottom plot).

For the passive behavior the subject's arm is moved by the robot with no voluntary intervention from the subject. Therefore, the actual trajectory is close to the optimal trajectory and the actual distance to the target is always larger than the optimal distance due to the proportional-derivative nature of the controller for calculating the supporting force. During the active behavior the user can explore the space around the optimal trajectory without being constrained by the robot. He can also

move faster than the optimal velocity. If necessary, the controller guides the hand to the target position at the end of the movement. Figure 10 shows forces generated by the robot to support the movement. For the passive behavior there is a clear force in the direction of the target, ${}^{\Psi}F_z$, and forces in perpendicular directions are close to zero. On the other hand, during the active behavior there is a force in the direction of the target when the subject moves the hand more slowly then defined by the optimal trajectory and there are forces in perpendicular directions to damp the movement that is not directed toward the target. The active arm weight compensation is in general larger for passive than for active behavior. For the measurements presented here the parameters for adaptation of weight compensation were selected such as to allow noticeable changes within a single reaching movement.

4. DISCUSSION

To implement patient-cooperative control for a rehabilitation robot, a novel strategy that uses the minimal intervention principle was proposed. The proposed controller is not stiff in the sense that it imposes a trajectory for the patient's movement. The task is only specified as a final posture that the patient needs to reach. Compared to the trajectory-based control approach the proposed controller enables the subject to choose their preferred trajectory for accomplishing the task. The patient can in this way exploit the preserved neural control of the upper limb muscles. The target posture together with the initial posture is first used to compute an optimal time-based trajectory, which is later compared to the hand distance to the target to determine the support necessary to accomplish the task. The controller allows more freedom in choosing the movement path compared to the frequently used strategy in rehabilitation robots—the virtual tunnel approach—where a movement path is specified and an impedance controller is implemented around the path to allow deviations from the prescribed trajectory [16].

Due to the fact that gravity strongly influences the movement of the upper limbs, an adaptive gravity compensation control system was implemented. This allows automatic detection of the patient's performance and sets an appropriate weight compensation level for the arm to allow the patient to comfortably accomplish the reaching task. The same weight support system is used also for other tasks that do not necessarily use the proposed minimal intervention principle control strategy.

The controller was designed in a way to adapt to active, as well as passive patient behavior. This means that, the control approach can be used for rehabilitation of completely paralyzed extremities, on the one hand, and almost completely functional limbs, on the other hand. Due to its adaptive nature, the control system does not need any adjustments for different patients. Of course this is not completely true for the robot itself, which needs some minor segment length adjustments in order to adapt to the patient's size. However, the changes are only limited to upper and lower arm segment lengths and the height of the robot. The entire adjustment procedure takes only about 1 min.

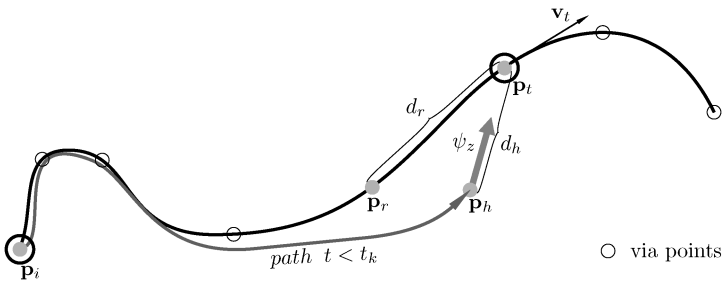

Figure 11. Controller with a continuous trajectory (for simplicity only the position part is shown): the target posture is not specified at the end of the trajectory, but it is rather moving along the trajectory with a velocity $\mathbf{v}_t$ at time t_k; the reference posture movement, which is following the target posture at an adaptable distance d_r, is governed by the minimum jerk strategy; the distance d_r is adapted based on the task requirements (i.e., the curvature of the path); the shorter d_r distance allows less freedom for the subject to choose his own path. Posture of the hand is always controlled within a sphere with radius d_r around the target point.

The drawback of the proposed implementation of the minimal intervention principle controller is the difficulty in coordinating the position and orientation of the hand during the movement itself. A discrete solution to this problem can be an introduction of via points that present intermediate targets. However, in this case, a smoothing of the force needs to be introduced in order to avoid step changes in the direction of the supporting force when switching from one to the other via point. On the other hand, these issues can be solved using a continuous solution as presented in Fig. 11.

In this case a movement trajectory is predefined (i.e., with a limited number of via points and a spline interpolation between them). Since the trajectory is specified in a continuous way, this makes it possible to coordinate position and orientation of the hand during the movement (i.e., when performing a complex task like moving a glass of water for drinking). However, the level of freedom that the patient has in planning their own trajectory can easily be adjusted. Compared to the basic control strategy presented in Fig. 2, where the target posture is predefined and constant, in the extended controller the target moves along a predefined trajectory. Its movement can be characterized by any simple principle not necessarily obeying the minimum jerk strategy. A simple strategy could be that the target posture moves along the complete trajectory in a predefined time slot to provide a time constraint for the patient's movement. Then a reference posture as in Fig. 2 is specified, which follows the target posture along the trajectory. However, the movement of the reference posture is governed by the minimum jerk strategy as defined in (14). Since both target and reference posture are moving in this case, it is possible to adapt the distance between them and in this way give the subject more or less freedom in planning his movement. Namely, based on the proposed control strategy (15), the patient's movement would be constrained to the predefined trajectory if the reference posture would exactly correspond to the target posture. In this case the patient could only move freely in a sphere with a radius zero around the target point.

By increasing the distance between the reference and the target posture, the patient would get more freedom in choosing their own trajectory within the sphere specified by the radius defined by the distance between the reference and the target posture. The strategy for adapting the distance between the two postures could be as simple as observing the curvature of the predefined trajectory and decreasing the distance when the radius of the curvature is small. In this way it would force the subject to follow the curve more precisely in the case of changes in the movement direction and leave more freedom for the patient on straight path segments. The distance between the reference and the target postures could also be adjusted based on the task specifications, i.e., by assessing the distance to possible obstacles (with smaller distance to an obstacle, the distance between the reference and the target postures would decrease) or by the importance of the coordinated position and orientation of the hand (when moving a glass filled with water). In all cases movement of the reference point is governed by the minimum jerk strategy, thus also constraining the movement of the patient's hand to a quasi-minimum jerk trajectory.

5. CONCLUSIONS

A novel paradigm for a patient-cooperative control strategy was proposed and evaluated. The strategy allows the patient to enforce their own movement trajectory for reaching movements, while the robot only supports their effort in order to complete the task. This is enabled by using the minimal intervention principle that exploits the redundancies in task execution. The patient's actions are not corrected unless they directly interfere with task specifications. The resulting movements are in general not optimal in terms of path lengths. However, the optimality can be observed on the level of jerk minimization. The optimization of path lengths is left to the patient through movement repetition. Some patients might never achieve optimal trajectories due to the lack of muscle coordination. However, they might still be able to reach the target using their own movement sequence with an adequate robot support and this is what the goal of the proposed control strategy is.

Acknowledgments

This work was partially supported by Marie Curie Intra European Fellowship MEIF-CT-2005-010084 to M. M.

REFERENCES

1. J. H. van der Lee, I. A. K. Snels, H. Beckerman and G. J. Lankhorst, Exercise therapy for arm function in stroke patients: a systematic review of randomized controlled trials, *Clin. Rehabil.* **15**, 20–31 (2001).
2. H. Woldag and H. Hummelsheim, Evidence-based physiotherapeutic concepts for improving arm and hand function in stroke patients, *J. Neurol.* **249**, 518–528 (2002).

3. C. Patten, J. Lexell and H. B. Brown, Weakness and strength training in persons with poststroke hemiplegia: rationale, method, and efficacy, *J. Rehabil. Res. Dev.* **41**, 293–312 (2004).
4. M. L. Aisen, H. I. Krebs, F. Mcdowell, N. Hogan and B. T. Volpe, The effect of robot assisted therapy and rehabilitative training on motor recovery following stroke, *Arch. Neurol.* **54**, 443–446 (1997).
5. N. Tejima, Rehabilitation robotics: a review, *Adv. Robotics* **14**, 551–564 (2000).
6. S. J. Biggs and M. A. Srinivasan, Haptic interfaces, in: *Handbook of Virtual Environments*, pp. 93–116. Earlbaum, New York, NY (2000).
7. W. S. Harwin and T. Rahman, Analysis of force-reflecting telerobotic system for rehabilitation applications, in: *Proc. 1st Eur. Conf. on Disability, Virtual Reality and Associated Technologies*, Maidenhead, pp. 171–178 (1996).
8. H. I. Krebs, N. Hogan, M. L. Alisen and B. T. Volpe, Robot-aided neurorehabilitation, *IEEE Trans. Rehabil. Eng.* **6**, 75–87 (1998).
9. R. Riener, T. Nef and G. Colombo, Robot-aided neurorehabilitation for the upper extremities, *Med. Biol. Eng. Comput.* **43**, 2–10 (2005).
10. B. Siciliano and L. Villani, *Robot Force Control*. Kluwer, Dordrecht (1999).
11. S. P. Gaskill and S. R. G. Went, Safety issues in modern applications of robots, *Rehabil. Eng. Syst. Safety* **53**, 301–307 (1996).
12. L. Schiavicco and B. Siciliano, *Modelling and Control of Robot Manipulators*. Springer, Berlin (2002).
13. J. H. Carr and R. B. Shepherd, *A Motor Relearning Programme for Stroke*. Butterworth, Oxford (1987).
14. J. H. Carr, R. B. Shepherd, A. M. Gentile and J. M. Held, *Movement Science. Foundations for Physical Therapy in Rehabilitation*. Aspen, Rockvil, MA (1987).
15. R. Shadmehr and F. A. Mussa-Ivaldi, Adaptive representation of dynamics during learning of motor task, *J. Neurosci.* **14**, 3208–3224 (1994).
16. R. Loureiro, F. Amirabdollahian, B. Driessen and W. Harwin, A novel method for computing natural path for robot assisted movements in synthetic worlds, in: *Proc. Assisitive Technology—Added Value to the Quality of Life*, Ljubljana, pp. 262–267 (2001).
17. E. Todorov and M. I. Jordan, Optimal feedback control as a theory of motor coordination, *Nat. Neurosci.* **5**, 1226–1235 (2002).
18. T. Flash and N. Hogan, The coordination of arm movements: an experimentally confirmed mathematical model, *J. Neurosci.* **5**, 1688–1703 (1985).
19. B. Hoff and M. A. Arbib, A model of the effects of speed, accuracy, and perturbation on visually guided reaching, *Exp. Brain Res.* **22**, 285–306 (1992).
20. D. A. Winter, *Biomechanics of Human Movement*. Wiley, New York (1979).
21. T. Nef and R. Riener, Armin—design of a novel arm rehabilitation robot, in: *Proc. 9th Int. Conf. on Rehabilitation Robotics*, Chicago, IL, pp. 57–60 (2005).
22. M. Mihelj, T. Nef and R. Riener, Armin—toward a six dof upper limb rehabilitation robot, in: *Proc. IEEE/RAS-EMBS Int. Conf. on Biomedical Robotics and Biomechatronics*, Pisa, CD-ROM (2006).

ABOUT THE AUTHORS

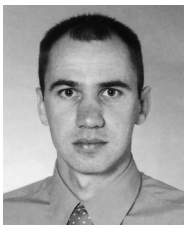

Matjaž Mihelj received the MS and DS degrees (1999 and 2002) in Electrical Engineering from the Faculty of Electrical Engineering, University of Ljubljana, Slovenia. Since 1998 has been a Teaching Assistant for Robotics and since 2003 he has been affiliated as an Assistant Professor at the Faculty of Electrical Engineering, University of Ljubljana. He gives lectures on man/machine interaction with the main focus on multimodal systems based on haptic devices. In 2001 he was a Visiting Researcher at Tohoku University, Sendai, Japan. From May 2005 to April 2006 he spent a year as a Visiting Researcher at the Automatic Control Laboratory of the Swiss Federal Institute of Technology (ETH Zurich). His research interests are in man/machine interaction, haptic interfaces as well as modeling and control of biological systems with the main focus on restoration of lost functions in people with disabilities.

Tobias Nef received the Dipl. Ing. degree in Electrical Engineering from the Swiss Federal Institute of Technology (ETH), Lausanne, Switzerland in 2002. He has been with the Sensory Motor Systems Group, ETH Zurich, Switzerland and at the Spinal Cord Injury Center at the University Hospital Balgrist, Zurich since 2003. For his work on the arm therapy robot ARMin, he received several awards including the humanTech Innovation Prize in 2005 and the Swiss Technology Award in 2006.

Robert Riener studied Mechanical Engineering at the TU München and the University of Maryland. He received a PhD degree in Electrical Engineering from the TU München in 1997. In 1993 he joined the Institute of Automatic Control Engineering, where he conducted research on modeling and control of neuroprostheses. After postdoctoral work from 1998 to 1999 at the Centro di Bioingegneria, Politecnico di Milano, he returned to the TU München, where he completed his Habilitation in the field of Biomechatronics in 2003. From 2003 to 2006 he was Assistant Professor of Rehabilitation Engineering at the Automatic Control Laboratory of the ETH Zurich and Spinal Cord Injury Center of the University Hospital Balgrist (double-professorship). Since June 2006, he has been Associate Professor for Sensory-Motor Systems at the Mechanical Engineering Department of ETH Zurich, while maintaining the double professorship with the University of Zurich. His research interests include human motion analysis, neuroprosthetics, biomechanics, haptic display technologies and rehabilitation robotics. He has authored and co-authored more than 150 peer-reviewed journal and conference articles as well as 13 patents. He was an Associate Editor of the *IEEE Transactions on Neural Systems and Rehabilitation Engineering* and Director of the International Functional Electrical Stimulation Society. Currently, he is an Editorial Member of three international journals and president of the AUTOMED society. He has received several awards including the Information Society Promotion Office Academic Challenge Award in 2003, the humanTech Innovation Prize in 2005 and the Swiss Technology Award in 2006.